DOI: 10.1002/chem.200700725

Zr-TUD-1: A Lewis Acidic, Three-Dimensional, Mesoporous, Zirconium-Containing Catalyst

Anand Ramanathan,[a, b, c] M. Carmen Castro Villalobos,[a, d] Cees Kwakernaak,[e] Selvedin Telalovic,[a] and Ulf Hanefeld*[a]

Dedicated to J. C. "Koos" Jansen, the inventor of TUD-1, on the occasion of his retirement

Abstract: A three-dimensional, mesoporous, silicate containing zirconium, Zr-TUD-1, was synthesized by a direct hydrothermal treatment method with triethanolamine as a complexing and templating reagent to ensure that zirconium was incorporated as isolated atoms. The mesoporosity of Zr-TUD-1 was confirmed by X-ray diffraction (XRD), N_2 sorption and high-resolution transmission electron micrograph (HR-TEM) studies. The nature and strength of the Lewis acid sites present in Zr-TUD-1 were evaluated by FTIR studies of pyridine adsorption and temperature-programmed desorption of ammonia. FTIR, X-ray photoelectron spectroscopic (XPS) and UV/Vis spectroscopic studies showed that, at Si/Zr ratios of 25 and higher, all the zirconium was tetrahedrally incorporated into the mesoporous framework, while at low Si/Zr ratios, a small part of the zirconium was present as ZrO_2 nanoparticles. Zr-TUD-1 is a Lewis acidic, stable and recyclable catalyst for the Meerwein–Ponndorf–Verley (MPV) reaction and for the Prins reaction.

Keywords: heterogeneous catalysis · isopulegol · Lewis acids · mesoporous materials · zirconium

Introduction

Lewis acids are versatile catalysts. They can promote the selective transfer of hydride ions in the reduction of ketones in the presence of carbon–carbon double bonds or in oxidations of alcohols as exemplified in the Meerwein–Ponndorf–Verley reduction/Oppenauer oxidation (MPVO reaction). In this reversible reaction that was first described as a reduction (Meerwein—Ponndorf–Verley), the Lewis acid aluminium(III) isopropoxide is commonly used in stochiometric quantities and recycling is difficult and often impossible.[1] Therefore, heterogeneous catalysts have been developed as an alternative.[2–5] The mechanism of both the homogenous and the heterogeneous MPVO reaction has been shown to proceed through a carbon-to-carbon hydride transfer from an alcohol to a ketone or aldehyde (Scheme 1).[6–8] The heterogeneous catalysts can also be used to racemise benzylic alcohols; in this case, however, the reaction occurs through an addition–elimination process.[6,9]

Moreover, Lewis acids catalyse such important reactions as the carbon–carbon bond forming Prins reaction. Prins described this reaction for the first time in 1917[10,11] and point-

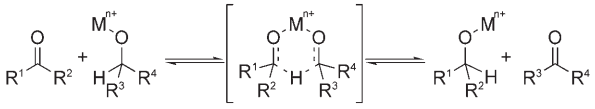

Scheme 1. The Lewis acid catalysed Meerwein–Ponndorf–Verley reduction/Oppenauer (MVPO) oxidation occurs through carbon-to-carbon hydride transfer.

[a] Dr. A. Ramanathan, Dr. M. C. Castro Villalobos, S. Telalovic, Dr. U. Hanefeld
Gebouw voor Scheikunde, Technische Universiteit Delft
Julianalaan 136, 2628 BL Delft (The Netherlands)
Fax: (+31) 15-278-1415
E-mail: U.Hanefeld@tudelft.nl

[b] Dr. A. Ramanathan
Advanced Chemical Technology Division
Korea Research Institute of Chemical Technology (KRICT)
P.O. Box 107, Yusung, Daejeon 305–600 (Republic of Korea)

[c] Dr. A. Ramanathan
Current address: Department of Chemistry
National Institute of Technology
Tiruchirappalli - 620015 (India)

[d] Dr. M. C. Castro Villalobos
Departamento de Tecnología Química y Ambiental
Universidad Rey Juan Carlos
Tulipán, s/n, 28933 Móstoles, Madrid (Spain)

[e] C. Kwakernaak
Department of Materials Science and Engineering
Technische Universiteit Delft, Mekelweg 2
2628 CD Delft (The Netherlands)

ed out that the cyclisation of citronellal to isopulegol (Scheme 2) described by him earlier that year[12] would also follow the same mechanism. This cyclisation is an essential step of the Takasago synthesis of menthol.[13] Industrially, this Prins reaction is catalysed by stochiometric amounts of

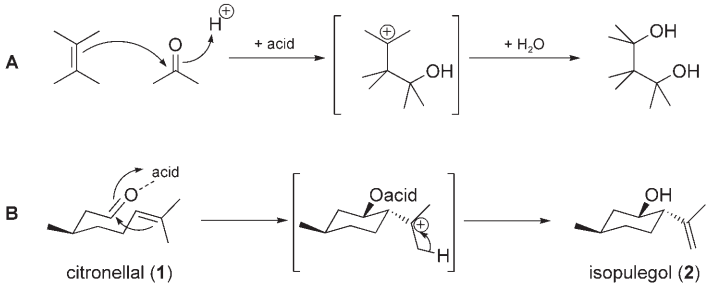

Scheme 2. A) In the acid-catalysed Prins reaction, a new carbon–carbon bond is formed between an olefin and an aldehyde, a propane-1,3-diol is produced. B) The cyclisation of citronellal (**1**) to isopulegol (**2**) follows the same mechanism.

solid $ZnBr_2$ in an organic solvent, originally benzene.[13,14] The $ZnBr_2$ can be replaced by very selective homogeneous catalysts, such as tris-(2,6-diarylphenoxy)aluminium,[15,16] that resemble MPVO catalysts.[1] The removal of homogeneous catalysts is, in general, cumbersome and introduces lengthy workup procedures.[17,18] Recently, the application of catalytic amounts of zeolites and mesoporous materials as catalysts for this reaction has attracted considerable attention.[19–27]

Since the discovery of MCM-41 mesoporous materials,[28] there has been tremendous development in the synthesis and modification of the silica framework. By virtue of their relatively large pores, mesoporous materials overcome the size and diffusion limitations that the microporous zeolites have. Acidity can be imparted to zeolites to obtain specific catalytic properties for a targeted reaction. For example, aluminium was incorporated to impart acidity[29–32], but other acidic metals such as zirconium also have this effect.[33–38] Zirconium is a particularly interesting metal, since tetrahedrally coordinated zirconium is only Lewis acidic and not Brønsted acidic.[8] In zirconia, zirconium has proven not only to be acidic,[39] but it has also been demonstrated to be very active in dehydration, hydrogenation, oxidation and hydride exchange reactions.[5,40] The very low surface area of zirconia was enlarged by supporting zirconium on silica and by the synthesis of both microporous and mesoporous materials in which the framework is substituted with zirconium. The presence of tetrahedrally incorporated Zr^{4+} in the framework makes them Lewis acidic. Indeed these materials can catalyse both the MPVO reaction and the Prins reaction.[25,33] As has recently been shown for Zr-beta, it is the LUMO d_{z^2} orbital of zirconium that accepts electron density from a Lewis base,[8] the zirconium remaining tetrahedrally coordinated in the framework. In both the Prins and the MPVO reaction, the Lewis base is identical: one of the lone electron pairs of the carbonyl group.

Consequently, the preparation of Zr-containing mesoporous materials is of great interest. However, the grafting of zirconium(IV) propoxide onto MCM-41, MCM-48 and SBA-15 is labour intensive.[33,38] Furthermore, several of the zirconium-containing mesoporous materials are one-dimensional, hence diffusion problems might once again arise.[37,41] A less labour intensive preparation of zirconium-containing mesoporous silicate again yields a material with a one-dimensional pore structure that limits diffusion.[42] Hence, the mesoporous materials prepared so far are either not readily accessible and/or one-dimensional. Both disadvantages need to be overcome in order to provide a straightforward catalytic system.

The recently reported three-dimensional sponge-like mesoporous material TUD-1[43] has many advantages over the conventional mesoporous materials HMS, MCM-41 and MCM-48, such as a cost-effective one-pot synthesis procedure, a tunable pore size and a better accessibility for substrates and products. These properties of TUD-1 are ideal for the incorporation of zirconium into the three-dimensional silica network either as isolated species or as zirconia clusters supported on the pore walls of TUD-1, depending on the Zr-loading. Earlier studies with other metals including zirconium indicated that, at loadings of up to 4%, the metal atoms are isolated in the framework of TUD-1.[44–51] In the synthesis of Ti-TUD-1, triethanolamine was demonstrated to be an ideal complexing agent for titanium.[44] Indeed, this complex and also the zirconium complex were isolated and fully characterised by others.[52] Triethanolamine thus ensured the incorporation of titanium as isolated atoms into the silica framework of Ti-TUD-1. It proved to act similarly in the synthesis mixtures of many other M-TUD-1s (M = metal) and specifically of Zr-TUD-1.[51] Thus, during the synthesis, no zirconia clusters can form and the metal is incorporated into the framework of the TUD-1 as an isolated atom. In this way, it is ensured that the metal is both isolated and fully accessible for the substrate. Independently, this triethanolamine approach was also developed for the preparation of Zr-MCM-41 and labelled as the "atrane route".[41,53,54] El Haskouri et al. demonstrated that triethanolamine complexes both silicon and zirconium atoms, ensuring the preparation of isolated metal sites in siliceous materials. Indeed, they could unambiguously show that both silicon and zirconium atrane complexes were present in an isolated form in the reaction mixture. Even when the two atranes were mixed, no silicon–silicon, zirconium–zirconium or bimetallic dimers were observed by fast atom bombardment mass spectrometry (FAB-MS), strongly indicating that the mesoporous materials are formed from monomeric atranes.[41,54] However, the materials prepared by this "atrane route" have the above-mentioned disadvantage of diffusion limitations, which are not present in the three-dimensional TUD-1. The sponge like character of TUD-1 was demonstrated, among others, by three-dimensional electron tomography studies.[55] Furthermore, M-TUD-1 has proven to be a particularly stable mesoporous material that can be recycled.[44–51]

In this paper, we report the direct, hydrothermal, cost-effective synthesis of zirconium-containing three-dimensional mesoporous silica Zr-TUD-1 with different Si/Zr ratios. A detailed characterisation of these materials obtained by different techniques such as X-ray diffraction (XRD), N_2 sorption, chemical analysis, high-resolution transmission electron micrographs (HR-TEM) and UV/Vis, FTIR and X-ray photoelectron spectroscopy (XPS) are discussed. These materials are evaluated for their Lewis acidic catalytic properties in the MPV reduction and the Prins reaction.

Results and Discussion

Zr-TUD-1 as a Lewis acidic, mesoporous material: A broad intense peak at low angle (0.4–2 θ) was observed in the X-ray powder diffraction pattern for all calcined Zr-TUD-1 samples (Figure 1) demonstrating the mesostructured character of these materials. No evidence for crystalline ZrO_2 was observed in the X-ray diffractograms, indicating that zirconium is incorporated into the framework. In line with the effects of metal loading in Co-TUD-1[46] and Al-TUD-1,[47] the peak intensity decreases slightly with an increase in the Zr loading, indicative of the influence of Zr loading on the integrity of the mesoporous structure. The HR-TEM of the sample Zr-TUD-1(25) (Figure 2, top) further confirms the mesoporosity. As expected, no crystalline zirconia particles were observed up to a loading of 4 mol% of zirconium in the TUD-1 matrix (Si/Zr = 25). However, at higher loadings, in Zr-TUD-1(10), a few crystalline nanoparticles were visible (Figure 2, bottom). The absence of zirconia crystals in the XRD-spectrum of the same sample indicates that the concentration of these nanoparticles must be low. The elemental analysis (ICP-OES) and porosity measurements obtained from N_2 sorption studies at 77 K are listed in Table 1. Elemental analysis indicated that the Si/Zr ratios in the calcined samples were the same as those in the initial synthesis

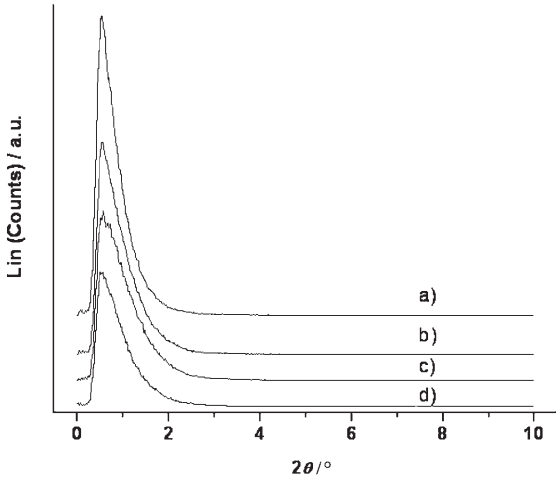

Figure 1. Powder X-ray diffraction patterns of a) Zr-TUD-1(100), b) Zr-TUD-1(50), c) Zr-TUD-1(25) and d) Zr-TUD-1(10).

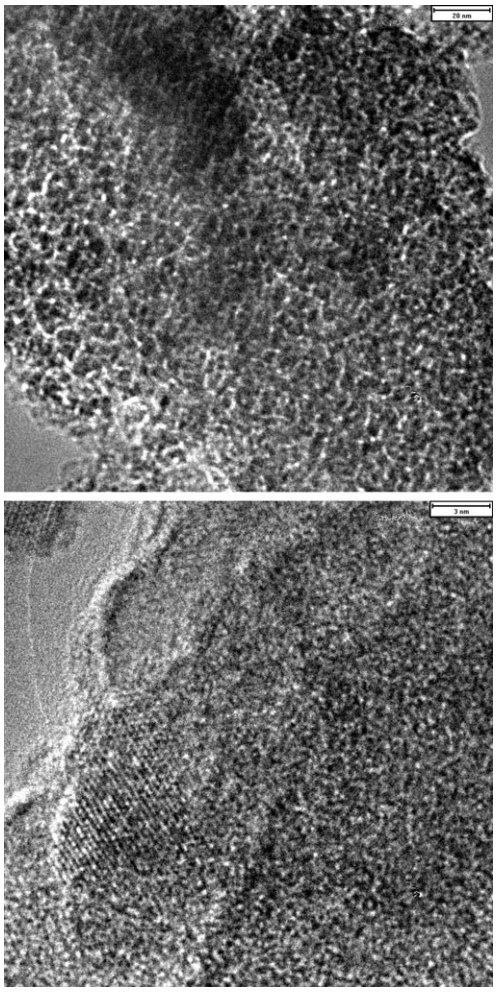

Figure 2. High-resolution transmission electron micrographs (HR-TEM) of calcined Zr-TUD-1 samples Zr-TUD-1(25) (top: bar represents 20 nm) and b) Zr-TUD-1(10) (bottom: bar represents 3 nm).

Table 1. Physicochemical characterisation of Zr-TUD-1 with different Zr loadings.

	Si/Zr ratio		S_{BET}	Total pore volume	Pore diameter	Micropore area	Micropore volume
	gel	product[a]	[$m^2 g^{-1}$]	[$cm^3 g^{-1}$]	[nm]	[$m^2 g^{-1}$])	[$cm^3 g^{-1}$]
Zr-TUD-1(10)	10	10	676	0.4	<2	n.a.	n.a.
Zr-TUD-1(25)	25	25	764	1.23	8.8	<1	<0.001
Zr-TUD-1(50)	50	51	771	1.2	8.9	32	0.009
Zr-TUD-1(100)	100	102	753	1.05	8	<1	<0.001

[a] From ICP-OES analysis.

gel. This excellent correlation of the Si/Zr ratio in the synthesis gel with that in the product demonstrates the high predictability of the synthesis method. This was also observed earlier for other M-TUD-1 materials.[46–48]

Three samples (Zr-TUD-1(100), Zr-TUD-1(50) and Zr-TUD-1(25)) show a type IV isotherm (Figure 3), indicated

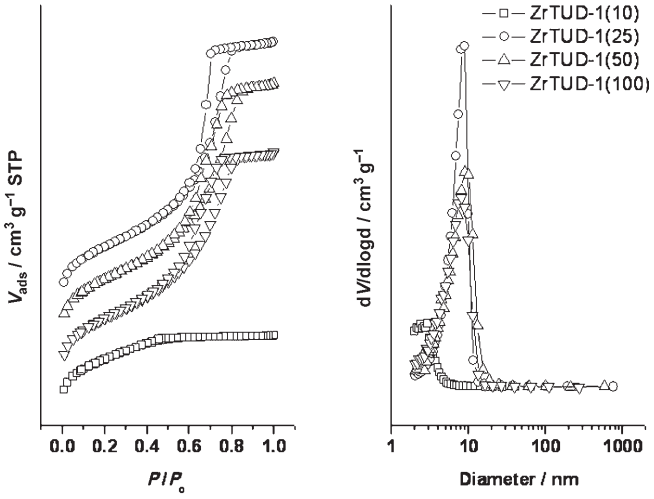

Figure 3. N_2 adsorption and desorption isotherms at 77 K and the corresponding pore size distribution of Zr-TUD-1 with different Zr loadings.

by the large uptake of nitrogen at relative pressures between 0.5 and 0.9 p/p_0 (due to capillary condensation in the mesopores). These samples also show a plateau at relative pressures above 0.9 p/p_0, indicating the absence of large mesopores, macropores or surface roughness in the measurable range (20 nm to approximately 500 nm). Additionally, these three samples have a larger pore size when compared to the all silica TUD-1 (ca. 4 nm). Presumably, this is due to the presence of the large zirconium atoms in the framework. The presence of some percolation or networking effects can also be deduced from a non-parallel adsorption and desorption isotherm.

Zr-TUD-1(10), on the other hand, showed an uptake of nitrogen at a relative pressure of up to approximately 0.5 p/p_0 and no adsorption is observed above this point. This implies the absence of large mesopores or macropores or surface roughness in the measurable range. Since pore filling occurs below the critical pressure of 0.43 p/p_0, no hysteresis was observed. This sample displayed very little mesoporosity and a maximum pore-size distribution below 2 nm. As a result of this, the pore volume is much lower than in the other three Zr-TUD-1 samples; however, the surface area of Zr-TUD-1(10) is comparable with the other three Zr-TUD-1 samples. The presumption that the large Zr-atom would cause an increase in pore size is not observed at this high concentration of zirconium. Instead, a differently structured material was formed with relatively small pores. This difference might be due to intensified interaction of the individual Zr atoms in the structure or due to the nanoparticles identified by HR-TEM.

From the XPS measurements, the observed binding energies of Zr $3d_{5/2}$ (183.2 ± 0.1 eV) presented in Table 2 differ significantly from the value reported for the reference sample ZrO_2 (182.4 eV), but are close to that of the reference sample $ZrSiO_4$ (183.3 eV).[56] The binding energy of O $1s_{1/2}$ observed at 532.4 ± 0.2 eV is also significantly higher

Table 2. The binding energy of the O $1s_{1/2}$, Zr $3d_{5/2}$ photoelectrons for Zr-TUD-1 samples.

Spectral line	Zr-TUD-1(10)	Zr-TUD-1(25)	Zr-TUD-1(100)
O $1s_{1/2}$	532.2	532.4	532.5
Zr $3d_{5/2}$	183.1	183.2	183.2

than both ZrO_2 (530.2 eV) and $ZrSiO_4$ (531.4 eV),[36,56] but approaches reported values of SiO_2 with values of about 532.9 eV as presented in the National Institute of Standards and Technology (NIST) X-ray Photoelectron Spectroscopy Database.[57] This is in line with the fact that all samples contain significantly more Si-O-Si bridges than Si-O-Zr bridges. Moreover, it indicates that the amount of ZrO_2 in Zr-TUD-1(10), although detectable by HR-TEM, is low. The binding-energy values for Zr $3d_{5/2}$ and O $1s_{1/2}$ are similar to those observed for Zr in the MFI structure,[58] zeolite beta[59] and mesoporous silicas.[56,60,61] These two observations are strong evidence for the presence of zirconium in the framework of the TUD-1 matrix, even in the case of Zr-TUD-1(10).

The IR spectra in the skeletal region of a KBr pressed disc of Si-TUD-1 and Zr-TUD-1 (Figure 4) showed typical

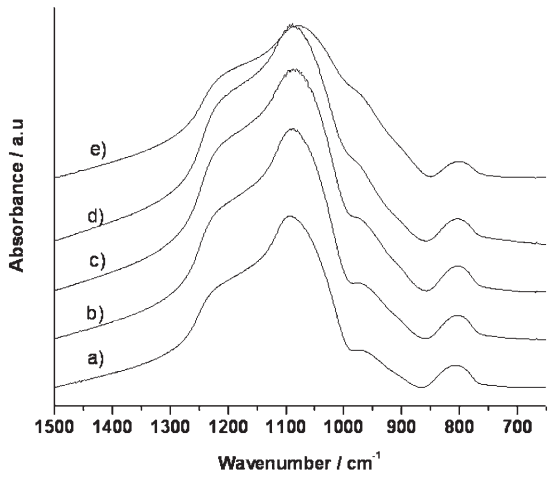

Figure 4. FTIR skeletal spectra a) Si-TUD-1, b) Zr-TUD-1(100), c) Zr-TUD-1(50), d) Zr-TUD-1(25) and e) Zr-TUD-1(10).

bands at 1093 cm^{-1} and a shoulder at 1220 cm^{-1} due to asymmetric stretching vibrations of Si-O-Si bridges and at 798 cm^{-1} due to symmetric stretching vibration of Si-O-Si.[35] The peak at 972 cm^{-1} (Si-TUD-1) is assigned to stretching vibrations of terminal silanol (Si-OH) groups present at defect sites.[62] In the Zr-TUD-1 samples, this peak is, to a

certain extent, due to Si-O-Zr stretching vibrations.[37,41,56] The presence of both of these vibrations leads to a relatively broad and less-resolved peak at 975 cm^{-1} in the case of the Zr-TUD-1 samples.

A temperature-programmed desorption (TPD) profile of ammonia for various Zr-TUD-1 samples showed a broad peak over the temperature range 120–500 °C (Figure 5). De-

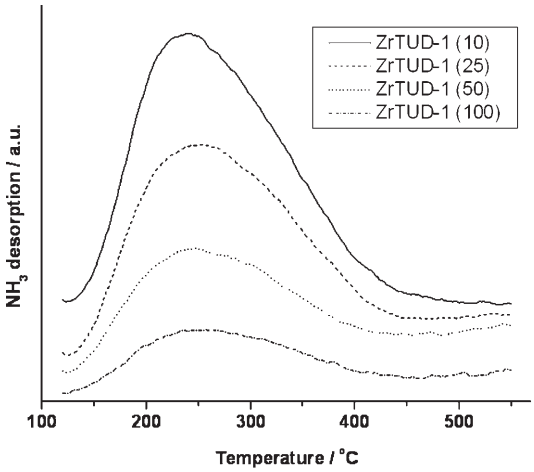

Figure 5. Temperature-programmed desorption (TPD) profile of ammonia for various Zr-TUD-1 samples.

convolution of this broad peak clearly shows three peaks corresponding to weak, medium and strong acid strength (Table 3). The total acidity of the samples follows the load-

Table 3. Acidity derived from temperature-programmed desorption (TPD) of ammonia for Zr-TUD-1 samples with different Si/Zr ratios.

Zr-TUD-1 (Si/Zr)	*T* [°C] (centre of deconvoluted peak)			mmol NH_3/g			Total acidity
	weak	medium	strong	weak[a]	medium[a]	strong[a]	
10	205	258	334	0.22	0.45	0.29	0.95
25	198	258	343	0.15	0.47	0.22	0.84
50	183	224	287	0.03	0.10	0.30	0.43
100	192	233	296	0.03	0.06	0.17	0.25

[a] Calculated from area of deconvoluted peak.

ing of zirconium: 0.954, 0.836, 0.433 and 0.247 mmol g^{-1} of ammonia for Zr-TUD-1 (10), Zr-TUD-1 (25), Zr-TUD-1 (50) and Zr-TUD-1 (100), respectively. The small difference between Zr-TUD-1 (10) and Zr-TUD-1 (25) is most likely due to the reduced surface area and the nanocrystals in Zr-TUD-1 (10) relative to the completely framework-incorporated zirconium in mesoporous Zr-TUD-1 (25).

FTIR spectra of both Si-TUD-1 and Zr-TUD-1 samples in the hydroxyl region (Figure 6) showed a band centred at 3745 cm^{-1}, which is attributed to terminal silanol groups. The intensity of this band decreases with the zirconium loading, indicating zirconium incorporation.[33] In addition, no band corresponding to terminal Zr–OH groups

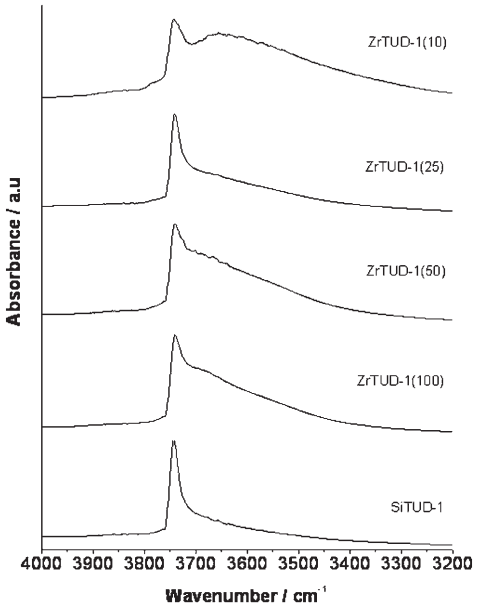

Figure 6. FTIR spectra in the OH group region of Si-TUD-1, Zr-TUD-1 (100), Zr-TUD-1 (50), Zr-TUD-1 (25) and Zr-TUD-1 (10).

(3780 cm^{-1}) as described by Jiménez-López et al. and Rakshe et al.[56,58] was detected for Zr-TUD-1 with Si/Zr = 25 or higher. This is good evidence that all the zirconium is tetrahedrally incorporated into the framework. Zr-TUD-1 (10) does have a week peak in this area; most likely the Zr–OH groups are due to the small amount of zirconia present in this material. All Zr-TUD-1 samples show a weak and broad shoulder at around 3650 cm^{-1}, which is due to Si–OH groups at defect sites.[33] This peak is strongest in the Zr-TUD-1 (10) sample, indicating that this material is less structured.

FTIR studies of adsorbed pyridine were carried out to access the type and strength of the acid sites. FTIR spectra of Zr-TUD-1 samples (Figure 7) after pyridine desorption at

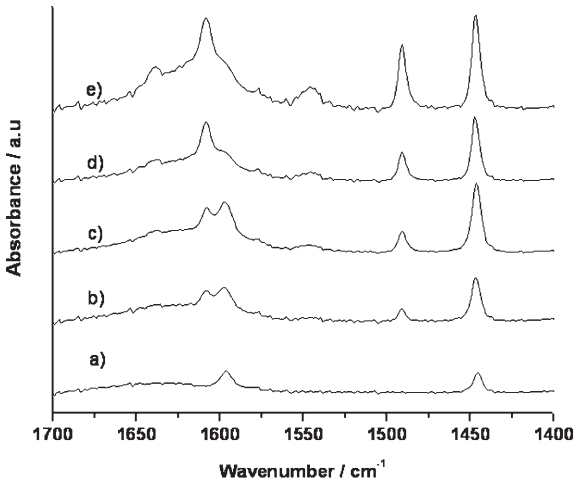

Figure 7. FTIR spectra of Si- and Zr-TUD-1 samples after pyridine desorption at 200 °C: a) Si-TUD-1, b) Zr-TUD-1 (100), c) Zr-TUD-1 (50), d) Zr-TUD-1 (25) and e) Zr-TUD-1 (10).

200 °C exhibits bands at ≈1610, 1547, 1447 and 1490 cm^{-1} corresponding to acid sites.[9,58,59] Pyridine coordinated to Lewis acid sites gives rise to two signals (≈1610 and 1447 cm^{-1}). A combination signal is associated with both Brønsted and Lewis acid sites (pyridinium ion and coordinated pyridine, respectively) at 1490 cm^{-1} and a signal indicative of only Brønsted acid sites (pyridinium ion at 1547 cm^{-1}). The bands at ≈1610 and 1447 cm^{-1} are present in higher intensity than in the reference material (Si-TUD-1) and increase with zirconium loading, proving the Lewis acidity of the materials. Moreover, the band at 1547 cm^{-1} is absent at low zirconium loading Si/Zr = 100) and very weak even at Si/Zr = 25. Only in Zr-TUD-1 (10) does this peak become more prominent. This might be due to Brønsted acidic sites of the zirconia particles in this sample or the Si–OH groups at defect sites. In other words, the increase in zirconium content up to Si/Zr = 25 induces Lewis acidity in the samples. Only traces of Brønsted acid sites were observed. This means that, as planned, zirconium induces the strong acid sites observed by NH_3–TPD and that these are due to Lewis acid sites. This is in line with the high Lewis acidity of Al-free Zr-beta and other zirconium-containing microporous silicates.[9,58,59]

Diffuse reflectance UV/Vis spectra of the Zr-TUD-1 samples showed, in each case, a weak and broad peak between 240 and 280 nm with a tail at around 350 nm (Figure 8). For

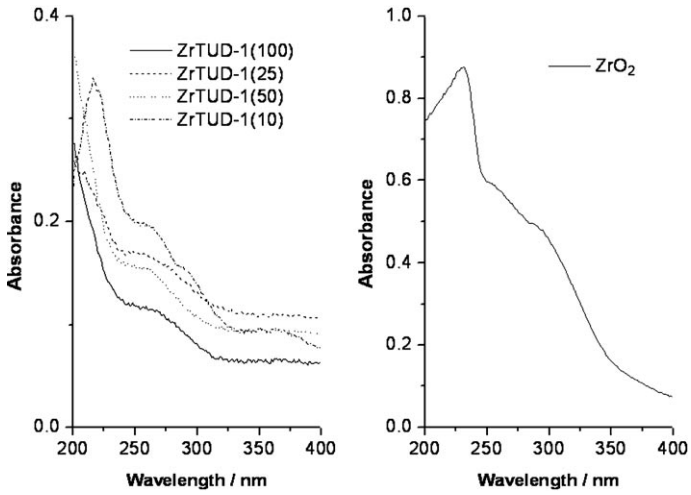

Figure 8. Diffuse reflectance UV/Vis spectra of various Zr-TUD-1 samples (left) compared with commercial ZrO_2 (right).

these samples, the peaks are assigned to $O^{2-} \rightarrow Zr^{4+}$ charge-transfer interactions with Zr in low coordination either isolated or present in small Zr_xO_y clusters in the silica network of TUD-1.[60] This is further supported by the fact that these spectra of Zr-TUD-1 (25), Zr-TUD-1 (50) and Zr-TUD-1 (100) were entirely different to the spectrum of commercial ZrO_2. Due to the low zirconium concentration, the expected signal at approximately 210 nm is not visible. The sample of Zr-TUD-1 (10) is different, since the spectrum displays a sharp band at 216 nm and the broad bands are slightly shifted to 260 and 340 nm. The band near 210 nm was assigned to the presence of isolated zirconium in a tetrahedral environment.[35,41] Again, similar to the XRD spectra, the zirconia nanoparticles visible in Zr-TUD-1 (10) by HR-TEM are not evident in the UV/Vis spectrum. This indicates that the concentration of zirconia nanoparticles must be very low.

Zr-TUD-1 as a Lewis acidic catalyst: Having established the tetrahedral nature of the isolated zirconium atoms in Zr-TUD-1, its catalytic activity was investigated in two acid-catalysed model reactions, the MPV reduction of 4-*tert*-butylcyclohexanone (**3**) (Scheme 3) and the carbon–carbon bond forming Prins reaction (Scheme 2).

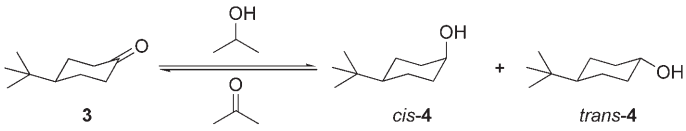

Scheme 3. The Zr-TUD-1 catalysed Meerwein–Ponndorf–Verley (MPV) reduction of 4-*tert*-butylcyclohexanone (**3**) proceeds diastereoselectively.

When the heterogeneous MPV reduction of 4-*tert*-butylcyclohexanone (**3**) is performed with zeolites such as H-beta,[2,63] Sn-beta[3,8] or Zr-beta,[4,5,8,59] a strong selectivity for the *cis* alcohol (*cis*-**4**) is observed. This high selectivity for the thermodynamically less favoured product is clearly related to the spatial confinement within the pores of the zeolite.[8] In mesoporous materials such as Zr-MCM-41, Zr-MCM-48 and Zr-SBA-15,[33] no spatial confinement is present and the thermodynamically determined dominance of the *trans* product (*trans*-**4**) is observed. Initial studies with Zr-TUD-1 and also Al-TUD-1 confirmed this behaviour.[51,64] However, Zr-TUD-1 (25) was not a very active catalyst under the originally described reaction conditions (2 mmol substrate in 4 mL isopropanol). Indeed, its activity was much lower than for the earlier reported Zr-MCM-41, Zr-MCM-48 and Zr-SBA-15,[33] although comparable reaction conditions were used. In an earlier study, the importance of the solvent in the homogeneous MPV reduction had been demonstrated.[65] Therefore, the Zr-TUD-1 (25) catalysed reduction of **3** was studied in coordinating and non-coordinating solvents (Figure 9). Alcohols coordinate well to the zirconium and thus block the active site, consequently *tert*-butyl alcohol inhibited the reaction (Table 4, entry 5). When the less coordinating ether 1,4-dioxane was

Table 4. Effect of the solvent on the MPV reduction of **3**.

	Solvent	**3**/isopropanol[a]	Conversion [%][b]	Selectivity [%]	*trans*-**4**/*cis*-**4**
1	isopropanol	1:26	83.0	>99	87:13
2	toluene	1:1	79.5	>99	76:24
3	toluene	1:3	97.5	>99	83:17
4	1,4-dioxane	1:1	37.3	>99	82:18
5	*tert*-butyl alcohol	1:1	4.54	>99	90:10

[a] Molar ratio. [b] After 3 days reaction at 80 °C.

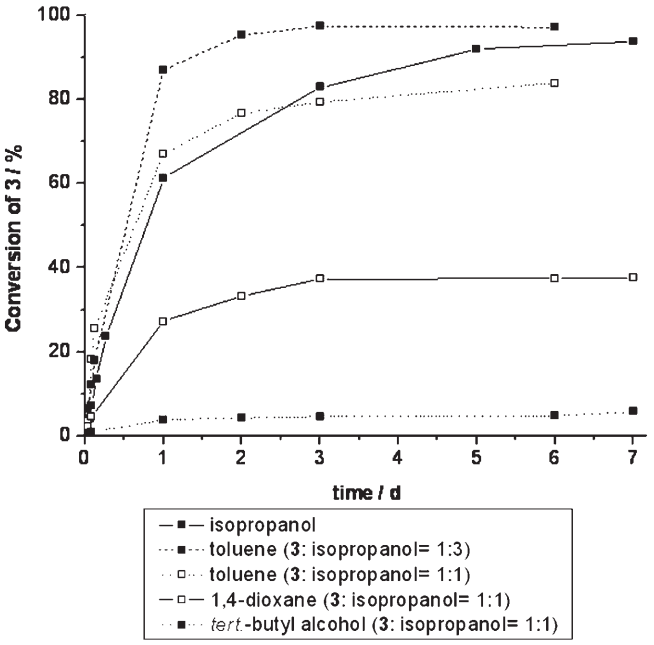

Figure 9. The solvent has a significant influence on the catalysts' activity in the MPV reduction of **3** (3.85 mL solvent, 50 mg Zr-TUD-1 (25), 80 °C).

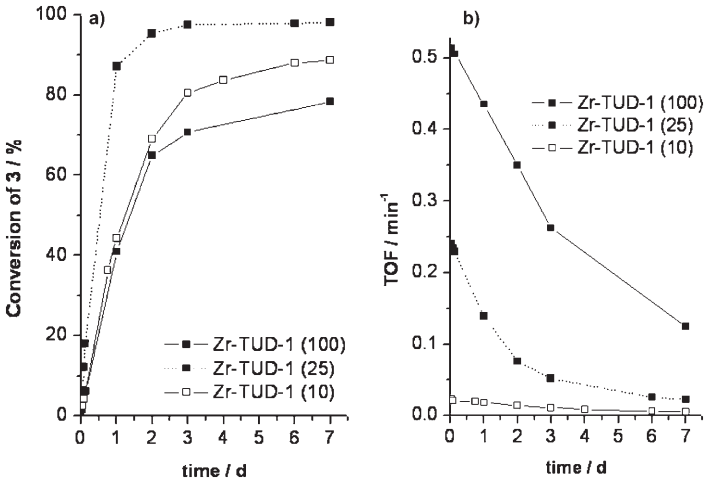

Figure 10. a) Conversion of **3** with Zr-TUD-1 (10), Zr-TUD-1 (25) and Zr-TUD-1 (100). b) TOF of Zr-TUD-1 (10), Zr-TUD-1 (25) and Zr-TUD-1 (100) in the reduction of **3** (TOF = mol **3** reacted mol Zr^{-1} min^{-1}) in toluene (3.55 mL) with three equivalents of isopropanol at 80 °C.

employed, the reaction proceeded faster than in *tert*-butyl alcohol (entry 4 versus 5). Toluene, however, did not inhibit the reaction. When three equivalents of isopropanol in toluene were used, the reactions proceeded smoothly (entries 2 and 3 versus 5). Isopropanol as a neat solvent inhibited the reaction due to coordination, too (entry 1) and, therefore, toluene was applied as the solvent. There seems to be little influence of the solvent on the *trans:cis* ratio of **4**, which is similar to results reported earlier for Zr-MCM-41, Zr-MCM-48 and Zr-SBA-15.

When Zr-TUD-1 with different Si/Zr ratios was employed for the MPV reduction, Zr-TUD-1 (25) displayed the highest activity per milligram of catalyst (Figure 10A). Evidently, the larger pore volume and diameter (Table 1) gives it an advantage over Zr-TUD-1 (10), which had a higher loading of Lewis acid sites. However, only the turn over frequency (TOF) reveals the true activity of the catalysts. The highest activity per catalytic site was observed for Zr-TUD-1 (100), clearly demonstrating that, as postulated above, no diffusion limitations occur in TUD-1 (Figure 10B). Again no influence on the *trans:cis* ratio of **4** ($\approx$83:17 for all the catalysts) was observed. Even though Zr-TUD-1 clearly displayed a much higher activity under these reaction conditions and accepts sterically very demanding substrates,[51] the overall activity was lower than that of comparable mesoporous zirconium-containing silicates.[33]

The acid-catalysed Prins reaction of citronellal (**1**) leads to cyclisation, yielding isopulegol (**2**) and its stereoisomers **5**–**7**. Due to its all-equatorial orientation of the substituents, **2** is the thermodynamically favoured product (Scheme 4).

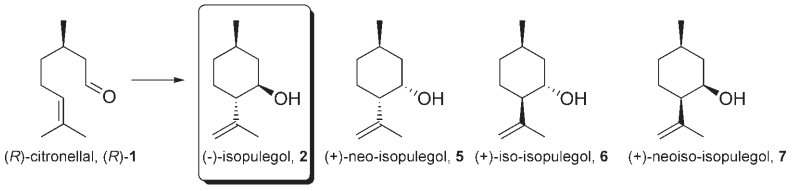

Scheme 4. Through the Prins reaction, citronellal (**1**) is cyclised to isopulegol (**2**) and its diastereoisomers **5**, **6** and **7**.

Similarly, based on the preferred all-equatorial transition state (Scheme 2B), it is also the kinetically favoured product.[20] In the first cyclisation studies performed with zeolites,[19,20] diastereoselectivities were low. Therefore, it was first proposed that the cyclisation takes place on the surface of the catalysts;[19] later calculations demonstrated that it can take place inside the pores of the zeolites.[20] Surprisingly, diastereoselectivities did not differ among the zeolites H-beta, H-MORD, H-ZSM-5 and H-Y[19,20,24,39] and mesoporous materials, although spatial confinement by the micropores of the zeolites might be expected to improve the stereoselectivity. With the introduction of tin and, in particular, zirconium into zeolite beta, the diastereoselectivity could be improved significantly, with Zr-beta being the catalyst of choice.[21,25,66] This superior selectivity was ascribed to the larger metal ion.[25] However, this improved selectivity is coupled to a reduced reactivity, possibly due to diffusion limitations.

Industrial grade *rac*-**1** (containing 6 % *rac*-**2**) was submitted to a Zr-TUD-1 (25)-catalysed Prins reaction at different temperatures in different solvents. As in the above-de-

scribed MPV reduction of **3**, coordinating solvents inhibited the reaction. In 1,4-dioxane, the reaction proceeded sluggishly but conversions >99% with selectivities >98% for the cyclisation products **2**, **5**, **6** and **7** were achieved at 80°C within two hours (Figure 11A). In toluene, the reaction proceeded significantly faster, and even at 40°C conversions >95% were realised within three hours with selectivities >98% for the cyclisation products **2**, **5**, **6** and **7** (Figure 11 B). Diastereoselectivities of **2**/(**5**+**6**+**7**) were always around 65:35. When compared to Zr-beta, a significant improvement in rate is observed, as might be expected in a virtually diffusion-limitation free material as TUD-1. Due to the lack of spatial confinement, the diastereoselectivity in Zr-TUD-1 is, however, lower than in Zr-beta. It might also be noted that, in contrast to our results, a coordinating solvent, namely *tert*-butyl alcohol, was the solvent of choice for Zr-beta.[25,66]

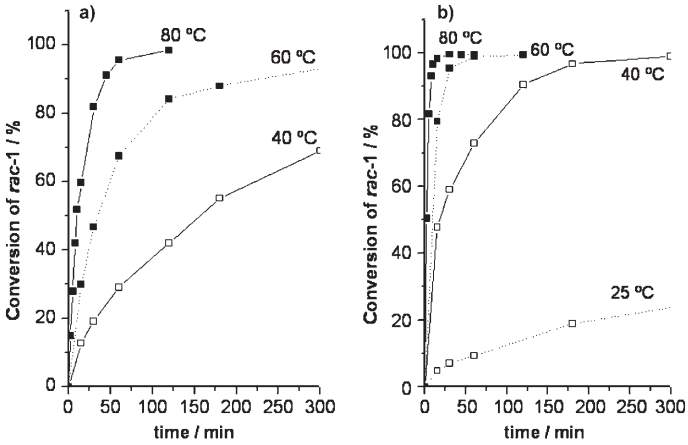

Figure 11. Cyclisation of industrial grade *rac*-**1** (2 mmol) catalysed by of Zr-TUD-1 (25) (50 mg) in a) 1,4-dioxane (4 mL) or b) toluene (4 mL) at different temperatures.

When Zr-TUD-1 with different Si/Zr ratios were compared for the cyclisation of *rac*-**1** in toluene, Zr-TUD-1 (25) had the highest activity per milligram of catalyst (Figure 12 A). Similar to the MPV reduction, the smaller pore diameter and pore volume (Table 1) of Zr-TUD-1 (10) reduced the activity of the Lewis acid sites significantly and the performance of Zr-TUD-1 (100) was even poorer. By determining the TOF, the real activity per active site was revealed (Figure 12B). Zr-TUD-1 (100) showed the highest TOF followed by Zr-TUD-1 (25). Clearly, this activity per active site of Zr-TUD-1 (100) in this very fast reaction was only possible due to the three-dimensional mesoporous character of the material that prevents diffusion limitations. The selectivity for the cyclisation of all three catalysts was (with >99%) excellent (Table 5). The diastereoselectivity towards **2** was always around 65:35; the reduced pore diameter of Zr-TUD-1 (10) did not have an influence on this ratio.

The stability of Zr-TUD-1 as a catalyst for the cyclisation of industrial grade *rac*-**1** containing approximately 6% of *rac*-**2** was established in a recycling experiment. Cycle times of 30 min were chosen in order to ensure that a possible loss of activity could be detected.[67] After five cycles, only a small loss of activity of the Zr-TUD-1 (25) was detectable (Figure 13). Given the crude nature of the starting material, the catalyst was calcined to remove any inhibitors contained in the feed. Full activity of the Zr-TUD-1 (25) was regained. In line with this, no leaching of zirconium could be detected (ICP-OES, detection limit 0.002 ppm). To confirm that the reaction was truly heterogeneous, hot filtration studies were performed. Upon removal of the catalyst at 80°C after 15 min of reaction (94% conversion), no further reaction was observed in the filtrate, confirming the heterogeneous nature of the catalysis.

The solvent studies for the MPV reduction had shown that alcohols could act as an inhibitor of Zr-TUD-1. As **2** and its diastereoisomers are alcohols, the cyclisation of **1** might be product inhibited. Since the crude *rac*-**1** contains *rac*-**2**, this might have been the reason for the observed loss of activity in the recycling experiments (Figure 13). Therefore, the Prins reaction of optically pure (+)-citronellal was compared with that of optically pure (+)-citronellal with 10% optically pure (−)-isopulegol (Figure 14, Table 6). The

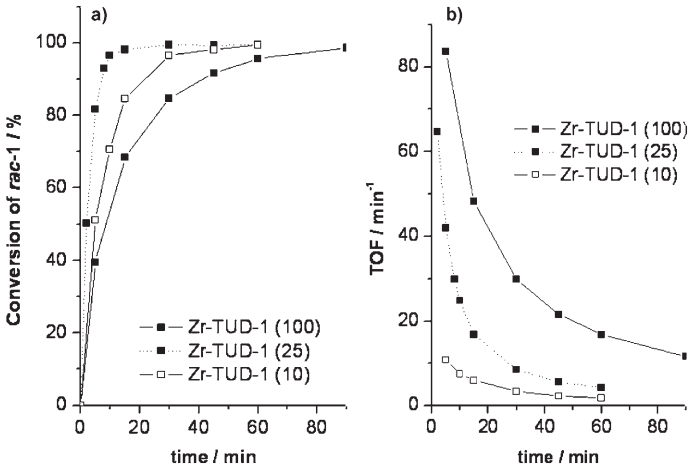

Figure 12. a) Cyclisation of industrial grade *rac*-**1** (2 mmol) catalysed by 50 mg Zr-TUD-1 (10), Zr-TUD-1 (25) or Zr-TUD-1 (100); b) TOF of Zr-TUD-1 (10), Zr-TUD-1 (25) and Zr-TUD-1 (100) in the cyclisation of industrial grade *rac*-**1** (TOF = mol **1** reacted mol Zr^{-1} min^{-1}) in toluene (4 mL) at 80°C.

Table 5. Cyclisation of industrial grade *rac*-**1** (2 mmol) catalysed by 50 mg Zr-TUD-1 (10), Zr-TUD-1 (25) or Zr-TUD-1 (100) in toluene (4 mL) at 80°C.

Catalyst	*t* [min]	Conversion [%]	Selectivity [%]	Molar ratio of isomers **2**/**5**/**6**/**7**
Zr-TUD-1 (10)	30	96.6	99.6	64.9:26.7:5.8:2.6
Zr-TUD-1 (25)	30	99.5	99.5	63.7:28.2:5.2:2.8
Zr-TUD-1 (100)	30	84.7	91.2	63.1:30.0:4.9:2.3
Zr-TUD-1 (10)	60	99.4	99.5	69.4:22.9:5.4:2.3
Zr-TUD-1 (25)	60	99.5	99.5	64.1:27.3:5.8:2.8
Zr-TUD-1 (100)	60	95.5	99.6	61.7:29.2:6.0:3.0

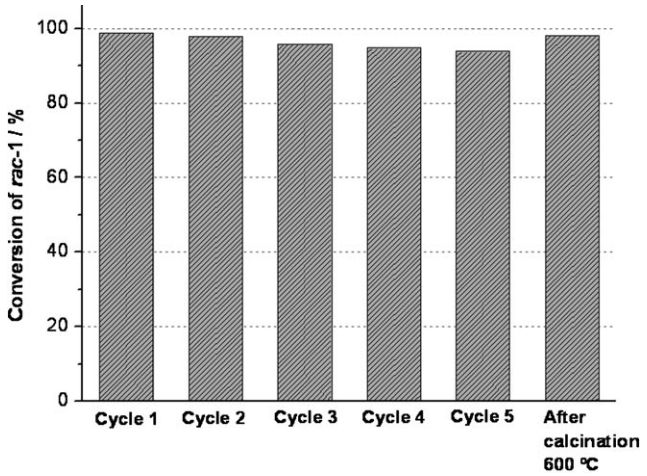

Figure 13. Recycling experiments with Zr-TUD-1 (25) (50 mg) in the cyclisation of industrial grade *rac*-**1** (2 mmol) in toluene (4 mL) at 80 °C, 30 min per cycle.

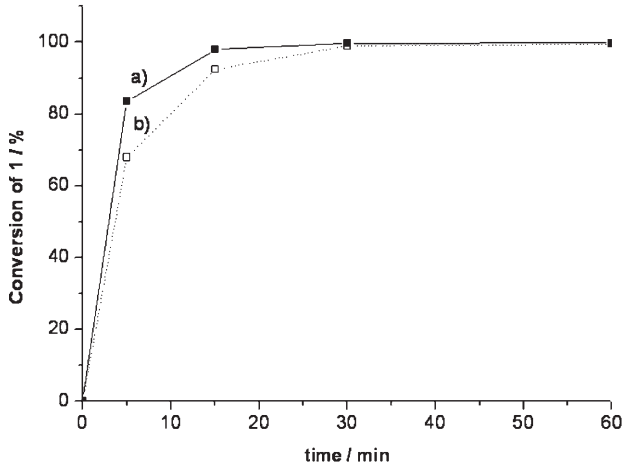

Figure 14. Cyclisation of a) (+)-**1** (2 mmol) and b) (+)-**1** (2 mmol) containing 0.2 mmol (−)-**2** catalysed by Zr-TUD-1 (25) (50 mg) in toluene (4 mL) at 80 °C.

Table 6. Initial rates for the cyclisation of (+)-**1** (2 mmol) and (+)-**1** (2 mmol) containing (−)-**2** (0.2 mmol) when catalysed by Zr-TUD-1 (25) (50 mg) in toluene (4 mL) at 80 °C.

	Initial rate [mmol mL^{-1} min^{-1}]
(+)-citronellal	0.075
(+)-citronellal + (−)-isopulegol	0.061

initial rates in the Zr-TUD-1 (25) catalysed reaction were different, the reaction containing product being slower. Compound **2** inhibited its formation from **1**. This product inhibition contributed to the reversible deactivation of Zr-TUD-1 as was observed in the recycling experiments.

Conclusion

The straightforward synthesis of a zirconium incorporated three-dimensional mesoporous silicate, Zr-TUD-1, with different Si/Zr ratios was achieved by means of a direct hydrothermal method with triethanolamine as the template. This is significantly more efficient than the grafting approach described for Zr-MCM-41, Zr-MCM-48 and Zr-SBA-15,[33] and of similar ease to the preparation of one-dimensional Zr-MPS carriers that were used as support for Fischer–Tropsch catalysts.[42] Zr-TUD-1 was shown to possess a high surface area, and no detectable zirconia phase was observed both in XRD and TEM for Si/Zr ratios of 25 and higher. Further increase in Zr content led to the formation of some ZrO_2 nanoparticles and some loss of mesoporosity evidenced by TEM and N_2 sorption studies. The framework incorporation of Zr at all concentrations was evident from FTIR, XPS and UV/Vis studies. Thus, a highly predictable and short synthesis of a novel mesoporous silicate with Zr incorporated into its framework was achieved. The properties of these materials such as high surface area, pore sizes similar to Si-TUD-1 and high Lewis acidity mean that Zr-TUD-1 can be utilized as a purely Lewis acidic catalyst for a variety of reactions.

Zr-TUD-1 was tested in the MPV reduction of 4-*tert*-butylcyclohexanone (**3**) and in the carbon–carbon bond forming Prins reaction. In the MPV reduction and in the Prins reaction, a clear solvent dependence of the catalytic activity was observed, with non-coordinating toluene being the solvent of choice. While the selectivity for the MPV reduction of **3** was excellent, the *trans* diastereoselectivity in this reduction was, as expected for a mesoporous material, low. In the Prins cyclisation of citronellal (**1**) to isopulegol (**2**), Zr-TUD-1 revealed its full catalytic potential. Both conversion of **1** and selectivity for the Prins cyclisation were >99%. Due to the three-dimensional sponge-like pore structure of Zr-TUD-1, no diffusion limitations were observed. Accordingly, Zr-TUD-1 has a very high activity, which is particularly evident when comparing the TOFs of the different Zr-TUD-1s; Zr-TUD-1 (100) had the most active catalytic sites (Figure 12B). While the diastereoselectivity of Zr-TUD-1 still needs to be improved, recycling experiments with industrial grade citronellal (**1**) demonstrated the great stability of Zr-TUD-1; any reversible loss of activity was due product inhibition. This stability was underlined by the fact that no leaching of zirconium could be detected. As a result, the new, readily prepared, three-dimensional, Lewis acidic Zr-TUD-1 is a promising catalyst for the Prins reaction.

Experimental Section

Synthesis of Zr-TUD-1: Zr-TUD-1 was synthesized with triethanolamine (TEA) as chelating agent in a one-pot procedure based on the sol–gel technique. Zr-TUD-1 with different Si/Zr atomic ratios was synthesized by adding appropriate amounts of tetraethyl orthosilicate (TEOS, 98%, Aldrich) to zirconium(IV) propoxide (Aldrich, 70 wt.% in 1-propanol) and of 2-propanol (30 mL). After stirring for a few minutes, appropriate amounts of a mixture of TEA (97%, ACROS) and water was added fol-

lowed by addition of tetraethyl ammonium hydroxide (TEAOH, 35 wt%, Aldrich) as a mineraliser under vigorous stirring. This yielded a gel with a molar ratio of $SiO_2/x\,ZrO_2$/(0.3–0.5) TEAOH/(0.5–1) TEA/(10–20) H_2O. The clear gel obtained after these steps was then aged at room temperature for 12–24 h, dried at 98 °C for 12–24 h, followed by hydrothermal treatment in a Teflon lined autoclave at 180 °C for 4–24 h and finally calcined in the presence of air up to 600 °C at a temperature ramp of 1 K min^{-1} and subsequent heating at 600 °C for 10 h. The Zr-TUD-1 obtained could be used for catalysis immediately or was, upon standing for a prolonged period of time, reactivated by repeating the calcination procedure. Samples with a Si to Zr ratio of 100, 50, 25 and 10 (denoted as Zr-TUD-1 (100), Zr-TUD-1 (50), Zr-TUD-1 (25) and Zr-TUD-1 (10), respectively) were prepared.

Material characterisation: Chemical analyses of Si and Zr were performed by dissolving the samples in an aqueous solution containing 1% HF and 1.3% H_2SO_4 and measuring them by inductively coupled plasma optical emission spectroscopy (ICP-OES) on a Perkin Elmer Optima 3000DV instrument. Powder XRD patterns were obtained on a Philips PW 1840 diffractometer equipped with a graphite monochromator using $Cu_{K\alpha}$ radiation. The textural parameters were evaluated from volumetric nitrogen physisorption at 77 K. Prior to the physisorption experiment, the samples were dried in vacuo at 300 °C, and the nitrogen adsorption and desorption isotherm was measured on a Quantachrome Autosorb-6B at 77 K. Transmission electron microscopy (TEM) was performed by using a Philips CM30T electron microscope with a LaB6 filament as the source of electrons operated at 300 kV. UV/Vis spectra were collected at room temperature on a Shimadzu UV-2450 spectrophotometer with $BaSO_4$ as reference.

Temperature-programmed desorption of ammonia measurements were carried out on a Micromeritics TPR/TPD 2900 equipped with a Thermal Conductivity Detector (TCD). The sample (30 mg) was pretreated at 550 °C in a flow of He (30 mL min^{-1}) for 1 h. Afterwards, pure NH_3 (40 mL min^{-1}) was adsorbed at 120 °C for 15 min. Subsequently, a flow of He (30 mL min^{-1}) was passed through the reactor for 30 minutes to remove any weakly adsorbed NH_3 from the sample. This procedure was repeated three times. Desorption of NH_3 was monitored in the range of 120 to 550 °C at a ramp of 10 K min^{-1}.

FTIR spectra of self-supported wafers and KBr-diluted wafers of Zr-TUD-1 samples were recorded on a Nicolet AVATAR 360 FTIR instrument. Skeletal FTIR spectra were carried out with KBr-diluted wafers in the region 1500–650 cm^{-1}. Acid-strength distribution was evaluated by IR spectra of adsorbed pyridine. It was carried out on self-supported wafers of Zr-TUD-1 samples (15–25 mg cm^{-2}) after evacuation (500 °C, 2 h, 10 Pa) in a custom made vacuum cell with CaF_2 windows. Then the cell was cooled down to room temperature, and the IR spectra were collected. As water and any adsorbed materials were removed by this treatment, hydroxyl spectra were obtained from this sample. Then, the temperature of the cell was raised to 100 °C, and the sample was then brought into contact with pyridine vapour (20 Torr) for 30 min. The temperature of the cell was raised to 150 °C, with vacuum applied for 30 min to remove physisorbed and loosely bound pyridine. Subsequently, the temperature of the cell was raised to 200 °C under vacuum for another 30 min. This procedure ensures the removal of all physisorbed pyridine (with only chemisorbed pyridine available for IR analysis). The cell was then cooled to room temperature, and the differential IR spectra were collected (Figure 7a). All of the spectra were recorded at room temperature with a resolution of 2 cm^{-1} averaged over 500 scans.

The XPS measurements were performed with a PHI 5400 ESCA provided with a dual Mg/Al anode X-ray source, a hemispherical capacitor analyser and a 5 keV ion gun. The input lens optical axis to the analyser was at a take off angle of 15° with respect to the sample surface normal. The input lens aperture used was 3.5 × 1.0 mm. All spectra were recorded with unmonochromated magnesium radiation. The X-ray source was operated at an acceleration voltage of 15 kV and a power of 400 W. A survey spectrum was recorded between 0 and 1000 eV binding energy with a pass energy of 71.95 eV and a step size of 0.25 eV. The spectra of the separate photoelectron and Si-Auger electron lines were recorded with a pass energy of 35.75 eV and a step size of 0.2 eV. The Zr-Auger electron line was recorded with a pass energy of 89.45 eV and a step size of 0.5 eV. The spectra were evaluated with Multipak 6.1 A software (Physical Electronics).

Catalytic experiments: All chemicals were purchased from Aldrich, Janssen or Acros. For the catalysis experiments, the anhydrous solvents and solids were used as received, all other liquids were dried and distilled prior to use. Zr-TUD-1 catalysts were activated in the presence of air at up to 600 °C at a temperature ramp of 1 K min^{-1} and subsequent heating at 600 °C for 10 h. The experiments were performed in dried glassware under a nitrogen atmosphere.

For the Meerwein–Ponndorf–Verley (MVP) reductions of 4-*tert*-butylcyclohexanone (**3**; 2 mmol), solvent and isopropanol (4 mL; e.g., 4 mL isopropanol or 3.85 mL solvent and 0.15 mL isopropanol = 2 mmol or 3.55 mL toluene and 0.45 mL isopropanol = 6 mmol) and 1,3,5-triisopropylbenzene (internal standard, 0.1 mL) were loaded into a Schlenk flask containing activated Zr-TUD-1 catalyst (50 mg). The reaction mixture was immediately immersed into an oil bath at 80 °C and the reaction was followed by taking samples of 20 μL. After the solvent screening, all MPV reductions of **3** were performed with toluene (3.55 mL) and isopropanol (0.45 mL), that is, with a ratio of **3** to isopropanol of 1:3, at 80 °C.

After one catalytic experiment, the catalyst was filtered off and the solvent evaporated. The *trans*:*cis* ratios of the 4-*tert*-butylcyclohexanols (**4**) obtained from this Meerwein—Ponndorf–Verley reduction of **3** was then established by ^{1}H NMR spectroscopy. The ^{1}H NMR spectrum of the mixture was recorded on a Varian-INOVA 300 MHz spectrometer in $CDCl_3$ with TMS as an internal standard and was in agreement with the literature spectra of *trans*-**4** and *cis*-**4**.[68] The ratio between *cis*-4-*tert*-butylcyclohexanol (*cis*-**4**) and *trans*-4-*tert*-butylcyclohexanol (*trans*-**4**) was determined from the well-separated signals of the H in the 1-position. For *cis*-**4** this H is equatorial and has a shift of $\delta = 4.032$ ppm, for *trans*-**4** this H is axial with a shift of $\delta = 3.510$ ppm. The *trans*:*cis* ratio for **4** was 83:17. Based on this analysis, the retention times for the diastereoisomers of **4** in the gas chromatography (GC) could be unambiguously assigned. Reactions were followed by GC with a Shimadzu GC-17 A gas chromatograph, equipped with a 25 m × 0.32 mm chiral column Chrompack Chirasil-Dex CB, split injector (1/97) at 220 °C, a Flame Ionisation Detector at 220 °C and He as carrier gas. The correct retention times observed (120 °C isotherm) are: 1,3,5-triisopropylbenzene (internal standard): 3.9 min; 4-*tert*-butylcyclohexanone (**3**): 4.7 min; *cis*-4-*tert*-butylcyclohexanol (*cis*-**4**): 5.6 min; *trans*-4-*tert*-butylcyclohexanol (*trans*-**4**): 5.9 min. The retention times previously reported in reference[51] accidentally give the reverse order for the diastereoisomers *cis*-**4** and *trans*-**4**. Under these conditions and with the correct assignment, the *trans*:*cis* ratio for **4** determined by ^{1}H NMR spectroscopy was confirmed. When the MPV reduction of **3** was performed with microporous H-beta as catalyst, the major product was *cis*-**4**[2] confirming the assignment of the retention times.

The Prins reaction experiments were carried out at 80, 60, 40 and 25 °C and using 50 mg of the catalyst. The reaction mixture consisted of 2 mmol of (±)-citronellal (*rac*-**1**) or enantiopure (+)-citronellal (+)-**1**, toluene or 1,4-dioxane (4 mL) as solvent and 1,3,5-triisopropylbenzene (internal standard, 0.1 mL). After the solvent and temperature screening, the ideal reaction conditions, 80 °C and toluene, were used. The reaction was followed by taking samples of 20 μL for GC analysis.

After one catalytic experiment, the catalyst was filtered off and the solvent evaporated. The ^{1}H NMR spectrum of the mixture was recorded on a Varian-INOVA 300 MHz spectrometer in [D_8]toluene with TMS as an internal standard. The spectrum of the main component (approx. 65% as determined by ^{1}H NMR spectroscopy, by using the signal of the H in the 1-position of **2** at 3.270 ppm) was identical to that of a commercial sample of **2**, while the other components were isomers **5**, **6** and **7**. Due to overlying signals, their separate concentrations could not be accurately determined. All other reactions were followed by GC. The samples obtained were analyzed with a VARIAN 1177 gas chromatograph equipped with an injector at 250 °C, a 30 m × 0.25 mm VARIAN FactorFour column and using a FID detector at 250 °C. The retention times observed (15 min 100 °C isotherm, then with a ramp of 100 K min^{-1} until 175 °C, then isotherm at 175 °C for 2 min) are: 1.4 min toluene, 4.8 min citronellal, 5.6 min neo-isopulegol, 6.1 min isopulegol, 6.4 min iso-isopulegol, 6.9 min

neoiso-isopulegol and 13.9 min 1,3,5-triisopropylbenzene. The products were identified on the basis of their retention times by comparison with commercial **1** and **2**. The other three isomers were assigned according to reference [20].

The recycling experiments of Zr-TUD-1(25) (50 mg) for the conversion of (±)-citronellal *rac*-**1** (2 mmol) in toluene (4 mL) as solvent and 1,3,5-triisopropylbenzene (internal standard, 0.1 mL) were performed at 80 °C for 30 min, then the catalyst was separated from the reaction mixture, dried and submitted to a new reaction. After the fifth cycle the Zr-TUD-1(25) was calcined at 600 °C before recycling. Results are given in Figure 13.

Acknowledgements

The authors would like to thank Dr. Ugo Lafont of DCT/NCHREM, Technische Universiteit Delft (The Netherlands), for performing the electron microscopy investigations. Financial support from NWO (Mozaïek fellowship) for S.T. is thankfully acknowledged. Stimulating discussions with Dr. J. A. Peters (TU Delft) are gratefully acknowledged. All this work would not have been possible without Dr. Koos Jansen, the inventor of TUD-1. We thank him for many fruitful discussions and advice.

[1] "Transfer Hydrogenation Including the Meerwein–Ponndorf–Verley Reduction": D. Klomp, J. A. Peters, U. Hanefeld, in *Handbook of Homogeneous Hydrogenation, Vol. 3* (Eds.: J. G. de Vries, C. J. Elsevier) Wiley-VCH, Weinheim, **2007**, Chapter 20, pp. 585–630.
[2] J. C. van der Waal, E. J. Creyghton, P. J. Kunkeler, K. Tan, H. van Bekkum, *Top. Catal.* **1997**, *4*, 261–268.
[3] A. Corma, M. E. Domine, S. Valencia, *J. Catal.* **2003**, *215*, 294–304.
[4] Y. Z. Zhu, G. K. Chuah, S. Jaenicke, *J. Catal.* **2006**, *241*, 25–33.
[5] G. K. Chuah, S. Jaenicke, Y. Z. Zhu, S. H. Liu, *Curr. Org. Chem.* **2006**, *10*, 1639–1654.
[6] D. Klomp, T. Maschmeyer, U. Hanefeld, J. A. Peters, *Chem. Eur. J.* **2004**, *10*, 2088–2093.
[7] R. Cohen, C. R. Graves, S.-B. T. Nguyen, J. M. L. Martin, M. A. Ratner, *J. Am. Chem. Soc.* **2004**, *126*, 14796–14803.
[8] M. Boronat, A. Corma, M. Renz, *J. Phys. Chem. B* **2006**, *110*, 21168–21174.
[9] Y. Z. Zhu, K. L. Fow, G. K. Chuah, S. Jaenicke, *Chem. Eur. J.* **2007**, *13*, 541–547.
[10] H. J. Prins, *Chem. Weekbl.* **1917**, *14*, 932–939.
[11] H. J. Prins, *Chem. Weekbl.* **1919**, *16*, 1072–1074.
[12] H. J. Prins, *Chem. Weekbl.* **1917**, *14*, 627–630.
[13] R. Noyori, *Adv. Synth. Catal.* **2003**, *345*, 15–32.
[14] Y. Nakatani, K. Kawashima, *Synthesis* **1978**, 147–148.
[15] T. Iwata, Y. Okeda, Y. Hori, US 6,774,269 B2, **2004**.
[16] M. Friedrich, K. Ebel, N. Götz, DE 10 2004 063 003 A1, **2006**.
[17] L. Veum, U. Hanefeld, *Chem. Commun.* **2006**, 825–831.
[18] R. A. Sheldon, I. Arends, U. Hanefeld, *Green Chemistry and Catalysis*, Wiley-VCH, Weinheim, **2007**.
[19] M. Fuentes, J. Magraner, C. de las Pozas, R. Roque-Malherbe, J. Perez Pariente, A. Corma, *Appl. Catal.* **1989**, *47*, 367–374.
[20] P. Mäki-Arvela, N. Kumar, V. Nieminen, R. Sjöholm, T. Salmi, D. Y. Murzin, *J. Catal.* **2004**, *225*, 155–169.
[21] A. Corma, M. Renz, *Chem. Commun.* **2004**, 550–551.
[22] F. Iosif, S. Coman, V. Pârvulescu, P. Grange, S. Delsarte, D. De Vos, P. Jacobs, *Chem. Commun.* **2004**, 1292–1293.
[23] D.-L. Shieh, C.-C. Tsai, C.-W. Chen, A.-N. Ko, *J. Chin. Chem. Soc.* **2003**, *50*, 853–860.
[24] D.-L. Shieh, C.-C. Tsai, A.-N. Ko, *React. Kinet. Catal. Lett.* **2003**, *79*, 381–389.
[25] Z. Yongzhong, N. Yuntong, S. Jaenicke, G.-K. Chuah, *J. Catal.* **2005**, *229*, 404–413.
[26] Y. Nie, G.-K. Chuah, S. Jaenicke, *Chem. Commun.* **2006**, 790–792.
[27] P. Mertens, F. Verpoort, A.-N. Parvulescu, D. De Vos, *J. Catal.* **2006**, *243*, 7–13.
[28] C. T. Kresge, M. E. Leonowicz, W. J. Roth, J. C. Vartuli, J. S. Beck, *Nature* **1992**, *359*, 710–712.
[29] D. Trong On, D. Desplantier-Giscard, C. Danumah, S. Kaliaguine, *Appl. Catal. A* **2001**, *222*, 299–357.
[30] R. Ryoo, S. Jun, J. M. Kim, M. J. Kim, *Chem. Commun.* **1997**, 2225–2226.
[31] R. Mokaya, W. Jones, *Phys. Chem. Chem. Phys.* **1999**, *1*, 207–213.
[32] B. Bonelli, B. Onida, J. D. Chen, A. Galarneau, F. Di Renzo, F. Fajula, E. Garrone, *Microporous Mesoporous Mater.* **2004**, *67*, 95–106.
[33] Y. Z. Zhu, S. Jaenicke, G.-K. Chuah, *J. Catal.* **2003**, *218*, 396–404.
[34] S. Gontier, A. Tuel, *Appl. Catal. A* **1996**, *143*, 125–135.
[35] M. S. Morey, G. D. Stucky, S. Schwarz, M. Fröba, *J. Phys. Chem. A* **1999**, *103*, 2037–2041.
[36] D. J. Jones, J. Jimenez-Jimenez, A. Jimenez-Lopez, P. Maireles-Torres, P. Olivera-Pastor, E. Rodrýguez-Castellon, J. Roziere, *Chem. Commun.* **1997**, 431–432.
[37] X. X. Wang, F. Lefebvre, J. Patarin, J. M. Basset, *Microporous Mesoporous Mater.* **2001**, *42*, 269–276.
[38] A. Tuel, *Microporous Mesoporous Mater.* **1999**, *27*, 151–169.
[39] G. K. Chuah, S. H. Liu, S. Jaenicke, L. J. Harrison, *J. Catal.* **2001**, *200*, 352–359.
[40] S. H. Liu, S. Jaenicke, G. K. Chuah, *J. Catal.* **2002**, *206*, 321–330.
[41] J. El Haskouri, S. Cabrera, C. Guillem, J. Latorre, A. Beltran, D. Beltran, M. Dolores Marcos, P. Amoros, *Chem. Mater.* **2002**, *14*, 5015–5022.
[42] M. Wie, K. Okabe, H. Arakawa, Y. Teraoka, *Catal. Commun.* **2004**, *5*, 597–603.
[43] J. C. Jansen, Z. Shan, L. Marchese, W. Zhou, N. van der Puil, T. Maschmeyer, *Chem. Commun.* **2001**, 713–714.
[44] Z. Shan, E. Gianotti, J. C. Jansen, J. A. Peters, L. Marchese, T. Maschmeyer, *Chem. Eur. J.* **2001**, *7*, 1437–1443.
[45] R. Anand, M. S. Hamdy, U. Hanefeld, T. Maschmeyer, *Catal. Lett.* **2004**, *95*, 113–117.
[46] M. S. Hamdy, A. Ramanathan, T. Maschmeyer, U. Hanefeld, J. C. Jansen, *Chem. Eur. J.* **2006**, *12*, 1782–1789.
[47] R. Anand, R. Maheswari, U. Hanefeld, *J. Catal.* **2006**, *242*, 82–91.
[48] M. S. Hamdy, G. Mul, W. Wei, R. Anand, U. Hanefeld, J. C. Jansen, J. A. Moulijn, *Catal. Today* **2005**, *110*, 264–271.
[49] M. S. Hamdy, G. Mul, J. C. Jansen, A. Ebaid, Z. Shan, A. R. Overweg, T. Maschmeyer, *Catal. Today* **2005**, *100*, 255–260.
[50] R. Anand, M. S. Hamdy, P. Gkourgkoulas, T. Maschmeyer, J. C. Jansen, U. Hanefeld, *Catal. Today* **2006**, *117*, 279–283.
[51] A. Ramanathan, D. Klomp, J. A. Peters, U. Hanefeld, *J. Mol. Catal. A* **2006**, *260*, 62–69.
[52] M. K. Sharma, A. Singh, R. C. Mehrotra, *Ind. J. Chem. Sect. A* **2001**, *40*, 568–572.
[53] S. Cabrera, J. El Haskouri, C. Guillem, J. Latorre, A. Beltran-Porter, D. Beltran-Porter, M. Dolores Marcos, P, Amoros, *Solid State Sci.* **2000**, *2*, 405–420.
[54] D. Ortiz de Zárate, A. Gómez-Moratalla, C. Guillem, A. Beltrán, J. Latorre, D. Beltrán, P. Amorós, *Eur. J. Inorg. Chem.* **2006**, 2572–2581.
[55] K. P. de Jong, A. J. Koster, A. H. Janssen, U. Ziese, *Stud. Surf. Sci. Catal.* **2005**, *157*, 225–242.
[56] A. Infantes-Molina, J. Mérida-Robles, P. Maireles-Torres, E. Finocchio, G. Busca, E. Rodríguez-Castellón, J. L. G. Fierro, A. Jiménez-López, *Microporous Mesoporous Mater.* **2004**, *75*, 23–32.
[57] C. D. Wagner, A. V. Naumkin, A. Kraut-Vass, J. W. Allison, C. J. Powell, J. R. Rumble, Jr., NIST X-ray Photoelectron Spectroscopy Database, Version 3.4 (Web Version) http://srdata.nist.gov/xps/, **2003**.
[58] B. Rakshe, V. Ramaswamy, S. G. Gegde, R. Vetrivel, A. V. Ramaswamy, *Catal. Lett.* **1997**, *45*, 41–50.
[59] Y. Zhu, G. Chuah, S. Jaenicke, *J. Catal.* **2004**, *227*, 1–10.

[60] E. Rodríguez-Castellón, A. Jiménez-López, P. Maireles-Torres, D. J. Jones, J. Rozière, M. Trombetta, G. Busca, M. Lenarda, L. Storaro, *J. Solid State Chem.* **2003**, *175*, 159–169.
[61] D. Fuentes-Perujo, S. Santamaria-Gonzalez, J. Merida-Robles, E. Rodríguez-Castellón, A. Jiménez-López, P. Maireles-Torres, R. Moreno-Tost, R. Mariscal, *J. Solid State Chem.* **2006**, *179*, 2182–2189.
[62] M. A. Camblor, A. Corma, J. Perez-Pariente, *J. Chem. Soc. Chem. Commun.* **1993**, 557–559.
[63] E. J. Creyghton, S. D. Ganeshie, R. S. Downing, H. van Bekkum, *J. Mol. Catal. A* **1997**, *115*, 457–472.
[64] In reference 51 the *trans:cis* ratio of **4** for the Zr-TUD-1 and Al-TUD-1 catalysed MPV reductions is accidentally reported as *cis:-trans* ratio.
[65] D. Klomp, K. Djanashvili, N. Cianfanelli Svennum, N. Chantapariyavat, C.-S. Wong, F. Vilela, T. Maschmeyer, J. A. Peters, U. Hanefeld, *Org. Biomol. Chem.* **2005**, *3*, 483–489.
[66] Y. Nie, W. Niah, S. Jaenicke, G. K. Chuah, *J. Catal.* **2007**, *248*, 1–10.
[67] C. Simons, U. Hanefeld, I. W. C. E. Arends, R. A. Sheldon, T. Maschmeyer, *Chem. Eur. J.* **2004**, *10*, 5829–5835.
[68] R. J. Abraham, J. J. Byrne, L. Griffiths, M. Perez, *Magn. Reson. Chem.* **2006**, *44*, 491–509.

Received: May 11, 2007
Published online: November 8, 2007

